Contribution from the Department of Chemistry, Merkert Chemistry Building, Boston College, 2609 Beacon Street, Chestnut Hill, Massachusetts 02167-3860, E. I. du Pont de Nemours and Company, Inc., Central Research and Development, Experimental Station, Wilmington, Delaware 19880-0328, and Du Pont Merck Pharmaceutical Company, Radiopharmaceutical Division, 331 Treble Cove Road, North Billerica, Massachusetts 01862

Ligand Addition Reactions and the Electron-Transfer Properties of $SnCl_2 \cdot 2H_2O$ and $SnCl_4 \cdot 5H_2O$. Molecular Structure of Bis(ethylcysteinato)tin(II)

J. E. Anderson,*,† S. M. Sawtelle,† J. S. Thompson,‡ S. A. Kretchmar Nguyen,§ and J. Calabrese∥

Received September 12, 1991

The synthesis and characterization of the tin(II) compounds Sn(ECD) and $Sn(CEE)_2$ and the tin(IV) complex $Sn(ECD)_2$, where H_2ECD is *N,N'*-1,2-ethylenediylbis(L-cysteine) diethyl ester and HCEE is L-cysteine ethyl ester, are reported. H_2ECD can be described in a general sense as a ligand with a N_2S_2 coordination site while the related complex HCEE has a NS coordination site following deprotonation of each thiol group on H_2ECD or HCEE. The crystal structure of $Sn(CEE)_2$ demonstrates that the N_2S_2 coordination scheme is adopted by tin(II) in these complexes. The crystal structure data for $Sn(CEE)_2[C_{10}H_{20}N_2O_4S_2Sn]$ are as follows: orthorhombic, space group $P2_12_12_1$, a = 5.582 (1) Å, b = 9.870 (1) Å, c = 28.886 (3) Å, V = 1591.5 Å^3, Z = 4, d_c = 1.732 g·cm^{-3}, μ(Mo) = 18.72 cm^{-1}, R = 0.027 (R_w = 0.030) for 252 parameters and 2324 unique reflections with $F_{o2} > 3\sigma(F_{o2})$. The speciation of $SnCl_2 \cdot 2H_2O$ and $SnCl_4 \cdot 5H_2O$ in the presence of either H_2ECD or HCEE was monitored by UV-visible and electrochemical methods, both of which demonstrate formation of a single product for tin(II) but multiple products for tin(IV). The electrochemical properties of $SnCl_2 \cdot 2H_2O$ and $SnCl_4 \cdot 5H_2O$ in water at a platinum electrode were measured and the effects of complexation by either H_2ECD or HCEE on the electrochemical response were examined. An adaptation of the chronocoulometric experiment was developed to examine the potential for oxidation of tin(II) to tin(IV), and this method has general applicability to systems characterized by EC electron-transfer mechanisms. The electrochemical properties of $Sn(ECD)Cl_2$ were also determined and compared with the electron-transfer properties of $SnCl_2 \cdot 2H_2O$ and $SnCl_4 \cdot 5H_2O$ in nonaqueous solvents.

Stannous chloride is used as a reducing agent for pertechnetate, TcO_4^-, in various radiopharmaceuticals.[1,2] The reduced Tc species is coordinated to ligands that direct the complex to target a specific organ, allowing imaging of that organ via the radioactive properties of technetium.[2] The complexation of the tin(II) reductant by ligands used for radiopharmaceutical applications and the effect that speciation has on the overall reducing ability of tin(II) has not been systematically investigated, even though complexation of a metal ion by a ligand results in significant changes in the potential for electron transfer.[3,4] The focus of the present study is to examine the speciation of tin(II) chloride and tin(IV) chloride with ligands that are relevant to radiopharmaceuticals and to examine the effect that speciation has on the reducing ability of the stannous complex.

In this paper we wish to report the reactions of tin(II) chloride and tin(IV) chloride with *N,N'*-1,2-ethylenediylbis(L-cysteine) diethyl ester (H_2ECD) and L-cysteine ethyl ester (HCEE). The

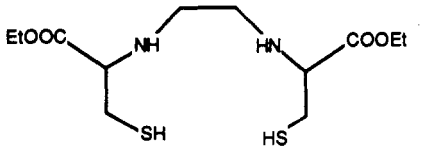

H_2ECD

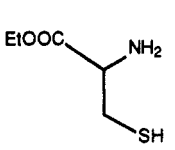

HCEE

radiopharmaceutical Neurolite, which is designed to image the brain, is based on the Tc(V) complex TcO(ECD) resulting from the reduction of pertechnetate with stannous chloride in the presence of H_2ECD.[5] H_2ECD provides a N_2S_2 coordination environment, whereas each HCEE ligand provides NS coordination, following deprotonation of the thiol groups. The coordination is confirmed in this report by the X-ray crystal structure of the Sn(II) complex $Sn(CEE)_2$. In general, the complexation reactions of tin(IV) species are significantly more complicated than those of tin(II) species.[1] For example, multiple tin(IV) products are often observed for a given reaction in which a single product is observed with stannous ion. The products from reaction of stannous and stannic chloride with H_2ECD and HCEE are consistent with this trend.

The redox properties of tin(II) and tin(IV) chloride and of the tin(II) and tin(IV) species from these reactions were studied by voltammetric techniques. Potentiometric and polarographic studies, primarily focused on the reduction of either tin(II) or tin(IV), constitute the majority of electrochemical data for tin in the literature.[6-8] Voltammetric examinations of the reduction of stannous and stannic ions have also been reported.[9-12] Until very recently,[13] the oxidative electrochemistry of tin(II) has not been well characterized, although studies with gold or carbon electrodes at high chloride concentrations have been reported.[9,14] The lack of data for the oxidation of tin(II) is due to inhibition of the electron-transfer process by adsorption of $SnCl_2$ onto the solid platinum or gold electrodes,[13] making observation of waves difficult with classical experiments. By modifying the chronocoulometry experiment,[15] we are able to examine the tin(II) to tin(IV) transition and examine how ligation effects this reaction. The methodology of this "new" technique will also be discussed, since in principle it could be used to study similar cases in which slow heterogeneous electron-transfer rates preclude normal electrochemical analysis.

Experimental Section

Materials. *N,N'*-1,2-Ethylenediylbis(L-cysteine) diethyl ester (H_2ECD) and $Sn(ECD)Cl_2$ were prepared by published procedures.[5,16,17]

† Boston College.
‡ E. I. du Pont de Nemours and Co., Inc. Contribution No. 5962.
§ Du Pont Merck Pharmaceutical Co. Current address: Salutar Imaging, 428 Oakmead Parkway, Sunnyvale, CA 94086.
∥ E. I. du Pont de Nemours and Co., Inc.

(1) Chemistry of Tin; Harrison, P. G., Ed.; Chapman and Hall, Inc.: New York, 1989; p 446.
(2) Clarke, M. J.; Fackler, P. H. *Struct. Bonding* **1982**, *50*, 60.
(3) For recent examples see ref 3 and 4: Lever, A. B. P. *Inorg. Chem.* **1990**, *29*, 1271.
(4) Lu, J.; Yamano, A.; Clarke, M. J. *Inorg. Chem.* **1990**, *29*, 3483.
(5) Edwards, D. S.; Cheeseman, E. H.; Watson, M. W.; Maheu, L. J.; Nguyen, S. A.; Dimitre, L.; Nason, T.; Watson, A. D.; Walovitch, R. *Technetium and Rhenium in Chemistry and Nuclear Medicine*; Cortinal International: Verona, Italy, 1990; Vol. 3, p 433.
(6) Galus, Z. *Encyclopedia of Electrochemistry of the Elements*; Bard, A., Ed.; J. Decker: New York, 1976; Vol. 4, p 223-271 (see also references therein).
(7) Lingane, J. J. *J. Am. Chem. Soc.* **1943**, *65*, 866.
(8) Bottari, E.; Liberti, A.; Rufolo, A. *J. Inorg. Nucl. Chem.* **1968**, *30*, 2173.
(9) Kadish, K. M.; Stamp, J.; Chemla, M.; Fatouros, N. *Anal. Lett.* **1973**, *6* (10), 909.
(10) Olson, C.; Adams, R. N. *Anal. Chim. Acta* **1963**, *29*, 358.
(11) Lerner, H.; Austin, L. G. *J. Electrochem. Soc.* **1965**, *112*, 636.
(12) Bard, A. J. *J. Electroanal. Chem.* **1962**, *3*, 117.
(13) Mandler, D.; Bard, A. J. *J. Electroanal. Chem.* **1991**, *307*, 217.
(14) Vincente, V. A.; Bruckenstein, S. *Anal. Chem.* **1972**, *44*, 297.
(15) Bard, A. J.; Faulkner, L. R. *Electrochemical Methods Fundamentals and Applications*; J. Wiley & Sons: New York, 1980; p 453.

0020-1669/92/1331-2778$03.00/0

L-Cysteine ethyl ester (HCEE) as the hydrochloride adduct, $SnCl_2 \cdot 2H_2O$, and $SnCl_4 \cdot 5H_2O$ were purchased from Aldrich and were used without further purification. For electroanalysis, spectroscopic grade acetonitrile and dichloromethane were purchased (Aldrich), purified by standard techniques,[18,19] stored over calcium hydride (CH_3CN) or phosphorus pentoxide (CH_2Cl_2) under inert atmosphere, and distilled just prior to use. Tetrabutylammonium perchlorate (TBAP) was purchased from Fluka, twice recrystallized from ethanol, and dried in a vacuum oven at 50 °C. Sodium perchlorate, $NaClO_4$, (99+%, Aldrich), NaCl (Aldrich), and HCl (Fisher Scientific) were purchased and used without further purification. Doubly deionized water from a Milli-Q water purification system was used for all aqueous studies.

Equipment and Techniques. Electrochemical experiments were performed with either a BAS-100A or an EG&G Princeton Applied Research Model 273 potentiostat/galvanostat coupled to an EG&G Princeton Applied Research Model RE0091-XY recorder and an IBM PS/2 Model 50 computer. A platinum-button working electrode, approximate area 0.008 cm^2, a platinum-wire counter electrode, and an SCE reference electrode separated from the solution with a bridge, comprised the three-electrode system for all voltammetric studies. For bulk electrolysis, a platinum-grid electrode, approximate area of 0.025 cm^2, a platinum-wire counter electrode and an SCE reference electrode separated from the solution with a bridge were the three-electrode system. The rotating disk studies were performed with an EG&G Princeton Applied Research Model 616 RDE. A large platinum electrode, approximate area 0.0125 cm^2, a platinum-wire counter electrode, and a silver-wire reference electrode were the three-electrode system. All potentials were measured vs a SCE reference electrode, and either ferrocene (for nonaqueous solutions) or $K_4Fe(CN)_6$ (for aqueous solutions) were used as internal standards. In the nonaqueous studies the supporting electrolyte was 0.1 M TBAP while for the aqueous studies the supporting electrolyte was 0.4 M $NaClO_4$, unless otherwise stated. The electrochemical cells were home built and designed for inert-atmosphere studies.[20] All aqueous solutions for electroanalysis were acidified to pH 2.0 with a 0.1000 M HCl standard solution, to avoid hydrolysis of the tin chloride species.[21]

NMR spectra were obtained on a GE QE-300 spectrometer; IR spectra were obtained on either a Nicolet 510 FT-IR spectrometer or a Perkin-Elmer 283B spectrometer. UV–visible spectra were obtained with either a Perkin-Elmer Lambda 3b or Lambda Array 3840 or a Hewlett Packard 8450A spectrometer.

Electrochemical Experimental Procedures. All manipulations for the electrochemical experiments followed standard Schlenk techniques,[22] that have been successfully used with highly air-sensitive organometallic compounds.[23] In addition, prior to electroanalysis, the supporting electrolyte and the analyte were degassed and dehydrated by applying vacuum for approximately 1.5 h and then back-filling with argon followed by three quick cycles of vacuum and back-filling. The electrochemical cells are thoroughly cleaned and stored in a 120 °C oven. The electrodes are cleaned in aqua regia, rinsed with water, and air-dried for at least 12 h prior to use.

Spectrophotometric Titrations. Separate solutions of $SnCl_2 \cdot 2H_2O$ and H_2ECD or HCEE with enough HCl to adjust the pH to 2.7 were prepared anaerobically under argon. Aliquots of $SnCl_2$ with increasing quantities of ligand (H_2ECD or HCEE) were transferred to an anaerobic quartz cuvette which had been purged with argon. After the reactions were completed (approximately 15 min) and no further increases in absorbance were observed as monitored by UV–vis spectroscopy, the UV–vis absorbance spectrum was recorded for each solution. Similar methods were used to study the tin(IV) complexation reactions, with the exception that significantly longer periods of time (approximately 4–5 h) were required to obtain stable spectroscopic data.

Preparation of $Sn^{IV}(ECD)Cl_2$. This complex was synthesized by published methods.[5]

Preparation of $Sn^{IV}(ECD)_2$. $H_2ECD \cdot 2HCl$ (0.78 g, 1.95 mmol) dissolved in water was added to $Sn(ECD)Cl_2$ (1.0 g, 1.95 mmol) dissolved in tetrahydrofuran. The solution was stirred for approximately 15 min, followed by addition of $NaHCO_3$ to raise the pH of the solution to 7.0, followed by extraction with CH_2Cl_2. The CH_2Cl_2 solution was then dried with Na_2SO_4, filtered, and evaporated to dryness to yield the crude product (as an oil). The oil was triturated three times with diethyl ether, evaporated to dryness each time, to yield a white product. The product was recrystallized with acetone–diethyl ether. Yield: 51%. Anal. (Galbraith) Calcd for $C_{24}H_{44}N_4S_4O_8Sn$: C, 37.75; H, 5.81; N, 7.19; S, 16.80; Sn, 15.55. Found: C, 37.28; H, 5.68; N, 7.34; S, 18.61; Sn, 15.36. Mass spectral results with chemical ionization (CH_4) confirmed formulation of the product as $Sn(ECD)_2$ by observation of parent peaks due to the isotopes of tin and the ionization method and by observation of relevant fragments.

Table I. Crystal Data for Bis(ethylcysteinato)tin(II)

molecular formula	$C_{10}H_{20}N_2O_4S_2Sn$
fw	415.10
cryst dimens, mm	0.40 × 0.20 × 0.35
space group	$P2_12_12_1$ (No. 18)
a, Å	5.582 (1)
b, Å	9.870 (1)
c, Å	28.886 (3)
V, Å^3	1591.5
Z	4
λ(Mo Kα radiation, from graphite monochromator), Å	0.71069
2θ limits, deg	1.4–60
temp, °C	−70
abs coeff, cm^{-1}	18.72
d_{calc}, $g \cdot cm^{-3}$	1.732
μ, cm^{-1}	18.72
transm factors	0.51–1.04
no. of data collcd	4966
no. of unique data used ($I > 3(\sigma)I$)	2324
R	0.027
R_w	0.030

Preparation of $Sn^{II}(ECD) \cdot HCl$. $H_2ECD \cdot 2HCl$ (0.20 g, 0.50 mmol), potassium carbonate (0.30 g, 2.2 mmol), and tin dichloride dihydrate (0.114 g, 0.50 mmol) were mixed as solids in a Schlenk flask. Deaerated distilled water (15 mL) was added under a nitrogen purge. The reaction mixture was stirred for 1.5 h and then extracted with 50 mL of deaerated dichloromethane. The organic layer was dried over magnesium sulfate and filtered to yield a clear filtrate. Removal of solvent and washing with petroleum ether yielded a white solid. Anal. (Galbraith) Calcd for $C_{12}H_{22}ClN_2S_2O_4Sn$: C, 30.17; H, 4.81; N, 5.86. Found: C, 30.16; H, 4.81; N, 5.64. ^1H NMR (ppm relative to internal tetramethylsilane) in dmso-d_6: 4.41 (broad singlet, 1 H), 4.14 (quartet, 2 H), 3.62 (broad singlet, 1 H), 2.95 (unsymmetrical multiplet, 4 H), 1.21 (triplet, 3 H).

Preparation of $Sn^{II}(CEE)_2$. L-Cysteine ethyl ester hydrochloride (0.50 g, 2.7 mmol) and potassium carbonate (0.77 g, 5.6 mmol) were dissolved in approximately 20 mL of deaerated deionized water under a nitrogen atmosphere. Tin dichloride dihydrate (0.304 g, 1.35 mmol) was added as a solid all at once. A white precipitate formed immediately. The reaction mixture was stirred for 0.5 h and then collected by suction filtration under nitrogen. The residue was washed extensively with deaerated deionized water. This solid was recrystallized from dichloromethane–diethyl ether. Anal. (Galbraith) Calcd for $C_{10}H_{20}N_2O_4S_2Sn$: C, 28.94; H, 4.86; N, 6.75. Found: C, 29.23; H, 4.80; H, 6.72. ^1H NMR (ppm relative to external tetramethylsilane) in dmso-d_6: 5.62 (broad singlet, 2 H), 4.15 (quartet, 2 H), 4.05 (multiplet, 1 H), 3.00 (unsymmetrical multiplet, 2 H), 1.22 (triplet, 3 H).

X-ray Data Collection and Structure Solution and Refinement for Bis(ethylcysteinato)tin(II). Crystals suitable for diffraction were obtained by vapor diffusion of diethyl ether into a dichloromethane solution of the complex under a nitrogen atmosphere. The crystal was encapsulated in a glass capillary, then was placed on an Enraf-Nonius CAD4 diffractometer, and was shown to be suitable for diffraction on the basis of ω scans, which showed the peak width at half-height to be ca. 0.18° ω at −70 °C. The cell parameters were then refined on the basis of 25 reflections chosen from diverse regions of reciprocal space. These parameters and other crystallographic data are summarized in Table I. Intensity data collection by the ω-scan technique, intensity measurements of standard reflections, and data processing were performed as described elsewhere.[24] Data were corrected for absorption (DIFABS) and for a 3% decrease in intensity. The structure was solved by automated Patterson analysis (PHASE). The minimized function is given elsewhere.[24] Atomic

(16) Walovtich, R. C.; Hill, T. C.; Garrity, S. T.; Cheeseman, E. H.; Burgess, B. A.; O'Leary, D. A.; Watson, A. D.; Ganey, M. V.; Morgan, R. A.; Williams, S. J. *J. Nucl. Med.* **1989**, *30*, 1892.
(17) Blondeau, P.; Berse, C.; Gravel, D. *Can. J. Chem.* **1967**, *45*, 49.
(18) Gordon, A. J.; Ford, R. A. *The Chemists Companion*; Wiley Interscience: New York, **1972**; p 408.
(19) Kadish, K. M.; Anderson, J. E. *Pure Appl. Chem.* **1987**, *59*, 5, 707.
(20) Anderson, J. E.; Sawtelle, S. M.; McAndrews, C. E. *Inorg. Chem.* **1990**, *29*, 2627.
(21) (a) Tobias, R. S. *Acta Chem. Scand.* **1958**, *12*, 198. (b) Imura, H.; Suzuki, N. *Anal. Chem. Acta* **1980**, *118*, 129.
(22) Shriver, D.; Drezdon, M. A. *The Manipulation of Air Sensitive Compounds*, 2nd ed.; Wiley Interscience: New York, 1986.
(23) Anderson, J. E.; Gregory, T. P. *Inorg. Chem.* **1989**, *28*, 3905.
(24) Thompson, J. S.; Harlow, R. L.; Whitney, J. F. *J. Am. Chem. Soc.* **1983**, *105*, 3522.

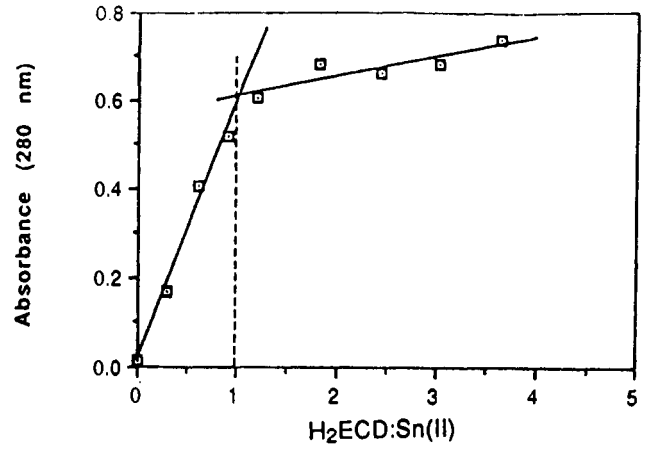

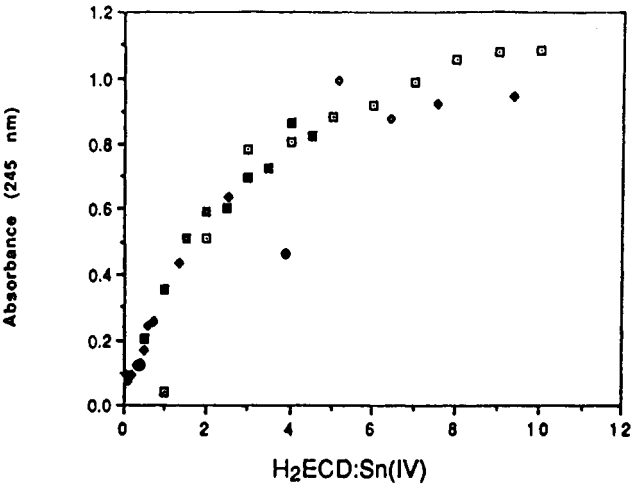

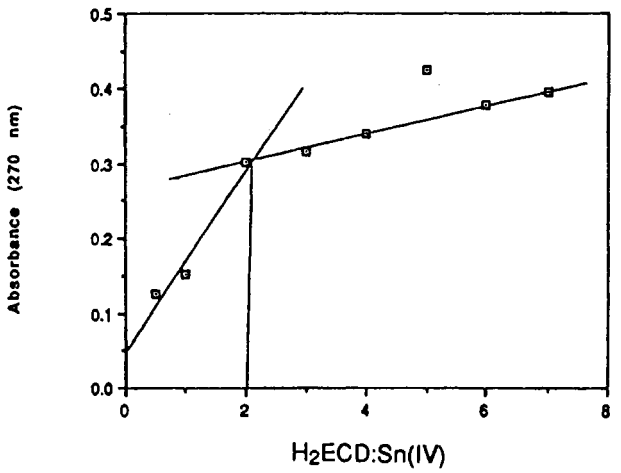

Figure 1. (a, Top) plot of absorbance (A) at λ = 280 nm vs the ratio of the concentration of H_2ECD to $SnCl_2 \cdot 2H_2O$ at pH = 2.7 demonstrating formation of a 1:1 complex. The initial concentration of $SnCl_2 \cdot 2H_2O$ was 2.65×10^{-4} M. (b, Middle) plot of absorbance (A) at λ = 245 nm vs the ratio of concentration of H_2ECD to $SnCl_4 \cdot 5H_2O$ at pH = 2.7. The initial concentration of $SnCl_4 \cdot 5H_2O$ was 3.59×10^{-4} M (c, Bottom) plot of absorbance (A) at λ = 270 nm vs the ratio of concentration of H_2ECD to $SnCl_4 \cdot 5H_2O$ at pH = 4.0 demonstrating formation of a 2:1 complex. The initial concentration of $SnCl_4 \cdot 5H_2O$ was 3.61×10^{-4} M.

scattering factors and anomalous dispersion terms were taken from the usual sources.[25] Least-squares refinement converged to R = 0.027 and R_w = 0.030 (R_w and w described elsewhere[24]). All peaks in the final difference Fourier map were less than or equal to 0.50 e/Å^3.

(25) (a) *International Tables for X-ray Crystallography*, Kynoch: Birmingham, England, 1974; Vol. IV, Table 2.2B. (b) *Ibid.*, Table 2.31.

Table II. Fractional Coordinates ($\times 10^4$) and Isotropic Thermal Parameters for Non-Hydrogen Atoms of Bis(ethylcysteinato)tin(II)

atom	x	y	z	B_{eq},[a] Å^2
Sn(1)	402.0 (5)	757.2 (3)	3045.3 (1)	2.0 (1)
S(1)	3766.7 (22)	43.3 (12)	2517.4 (4)	2.3 (1)
S(2)	1760 (2)	3118 (1)	3251	2.5 (1)
O(1)	−1629 (6)	2456 (4)	1397 (1)	3.1 (1)
O(1′)	1487 (8)	1181 (4)	4361 (1)	4.0 (1)
O(2)	2299 (6)	2688 (4)	1254 (1)	2.8 (1)
O(2′)	3602 (7)	3114 (4)	4399 (1)	3.3 (1)
N(1)	−800 (6)	1719 (4)	2314 (1)	2.2 (1)
N(1′)	3832 (8)	327 (4)	3602 (2)	2.5 (1)
C(1)	1235 (7)	1967 (4)	2004 (2)	1.8 (1)
C(1′)	4671 (10)	1567 (5)	3822 (2)	2.4 (1)
C(2)	2750 (7)	685 (4)	1961 (2)	2.1 (1)
C(2′)	4729 (10)	2721 (5)	3465 (2)	2.5 (1)
C(3)	402 (10)	2400 (4)	1524 (1)	2.1 (1)
C(3′)	3039 (10)	1907 (5)	4220 (2)	2.7 (1)
C(4)	1810 (13)	3066 (7)	779 (2)	3.4 (1)
C(4′)	2016 (14)	3637 (7)	4754 (2)	4.1 (2)
C(5)	3912 (13)	2714 (9)	493 (2)	4.4 (2)
C(5′)	−43 (14)	4367 (8)	4547 (3)	5.3 (2)

[a] $B_{eq} = {}^4/_3 S_i S_j b_{ij} a_i a_j$.

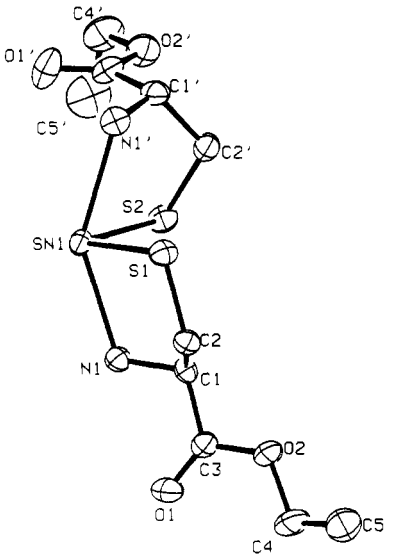

Figure 2. Crystal structure of bis(ethylcysteinato) tin(II), $Sn(CEE)_2$, with hydrogens removed for clarity.

Final positional parameters of the non-hydrogen atoms appear in Table II. Tables of complete crystallographic data, general temperature factors, hydrogen atom positions, structure factor amplitudes, and a complete listing of bond distances and angles are available as supplementary material.[26]

Results and Discussion

Ligand Addition Reactions to Tin(II) and Tin(IV) Chloride. The complexation reactions of aqueous tin(II) chloride with either H_2ECD or HCEE result in the formation of either Sn(ECD)·HCl or $Sn(CEE)_2$. These reactions were followed by UV–visible spectroscopy, and a typical result is shown in Figure 1a for the reaction of $SnCl_2 \cdot 2H_2O$ with H_2ECD at pH near 2.7. Neither the tin ion nor H_2ECD has a significant absorption at 280 nm, yet upon formation of a Sn–ECD complex the absorbance at 280 nm increases. By variation of the molar ratio of Sn to ECD while the absorbance at 280 nm is monitored and the resulting absorbance vs the ECD:Sn(II) ratio is plotted, the stoichiometry of the resulting complex was determined to be 1:1, as shown in Figure 1a. Similarly, titrations of tin(II) chloride with HCEE yielded a molar ratio of one tin to two CEE ligands. The results of the UV–vis titration experiments are in agreement with the synthetic results in which isolation of Sn(ECD) and $Sn(CEE)_2$ are observed.

(26) See paragraph at end of the paper regarding supplementary material.

Table III. Selected Bond Distances (Å) and Angles (deg) for Bis(ethylcysteinato)tin(II)

	Bond Distances		
Sn(1)–S(1)	2.520 (1)	O(1′)–C(3′)	1.195 (6)
Sn(1)–S(2)	2.521 (1)	O(2)–C(3)	1.346 (6)
Sn(1)–N(1)	2.412 (4)	O(2)–C(4)	1.448 (6)
Sn(1)–N(1′)	2.537 (4)	O(2′)–C(3′)	1.336 (6)
S(1)–C(2)	1.817 (5)	O(2′)–C(4′)	1.450 (7)
S(2)–C(2′)	1.811 (6)	N(1)–C(1)	1.467 (5)
O(1)–C(3)	1.193 (6)	N(1′)–C(1′)	1.457 (6)
	Bond Angles		
S(1)–Sn(1)–S(2)	100.19 (4)	O(1)–C(3)–O(2)	124.0 (4)
S(1)–Sn(1)–N(1)	77.7 (1)	O(1′)–C(3′)–O(2′)	125.0 (5)
S(1)–Sn(1)–N(1′)	77.0 (1)	O(1)–C(3)–C(1)	125.7 (4)
S(2)–Sn(1)–N(1)	85.8 (1)	O(2)–C(3)–C(1)	110.3 (4)
S(2)–Sn(1)–N(1′)	77.2 (1)	O(1′)–C(3′)–C(1′)	124.4 (5)
N(1)–Sn(1)–N(1′)	146.3 (1)	O(2′)–C(3′)–C(1′)	110.6 (4)
Sn(1)–S(1)–C(2)	101.8 (1)	O(2)–C(4)–C(5)	108.7 (5)
Sn(1)–S(2)–C(2′)	99.0 (2)	O(2′)–C(4′)–C(5′)	111.1 (5)
C(3)–O(2)–C(4)	117.1 (4)	N(1)–C(1)–C(2)	109.8 (3)
C(3′)–O(2′)–C(4′)	116.6 (5)	N(1)–C(1)–C(3)	111.4 (3)
Sn(1)–N(1)–C(1)	112.6 (3)	N(1′)–C(1′)–C(2′)	109.6 (4)
Sn(1)–N(1′)–C(1′)	112.2 (3)	N(1′)–C(1′)–C(3′)	109.0 (4)
S(1)–C(2)–C(1)	113.0 (3)	C(2)–C(1)–C(3)	109.2 (4)
S(2)–C(2′)–C(1′)	111.7 (4)	C(2′)–C(1′)–C(3′)	111.2 (4)

For both Sn(ECD) and $Sn(CEE)_2$, there is a N_2S_2 coordination scheme of the tin metal resulting in a typical four-coordinate species.[27]

The coordination of the tin ion in $Sn(CEE)_2$ is shown in Figure 2. The overall structure of this compound is a distorted four-coordinate pyramidal geometry due to the four ligand coordination sites and the "open" equatorial site occupied by the tin(II) lone pair. This geometry is common for four-coordinate Sn(II) complexes.[28] The two ligands coordinate to the stannous ion through the amine nitrogen atom and the thiolate sulfur atom. There is no interaction between the ester group of the CEE ligand and the metal ion.

Selected bond distances are presented in Table III. The average Sn–S distance of 2.52 Å is typical of stannous complexes while the average Sn–N distance of 2.48 Å is slightly longer than what has been previously reported.[29] Tin(II)–nitrogen bond distances typically range from 2.06 to 2.45 Å while tin(II)–sulfur distances range from approximately 2.20 to 2.70 Å. The two Sn–S distances are nearly identical, while there is considerable difference between the two distinct Sn–N distances of 2.41 and 2.54 Å. This difference in Sn–N bond distances result at least in part from a hydrogen-bonding interaction between N(1′) and O(1) in a neighboring molecule [N(1′)–O(1), 3.089 (6) Å]. There is no such interaction at N(1). The bond angles around the tin are representative of a distorted pyramidal structure. For example, the S–Sn–S and N–Sn–N bond angles are near 100 and 146°, respectively. Table III also lists selected bond angles.

The results of titration studies of tin(IV) and H_2ECD at pH = 2.7 are shown in Figure 1b, which plots the absorbance at 245 nm as a function of the H_2ECD:Sn(IV) ratio for five separate runs. The curvature in the plot indicates that multiple Sn(IV)–ECD species are present. The results are simplified at higher pH values, and under these conditions a 2:1 ECD to Sn(IV) complex is formed, as shown in Figure 1c. The 2:1 complex is

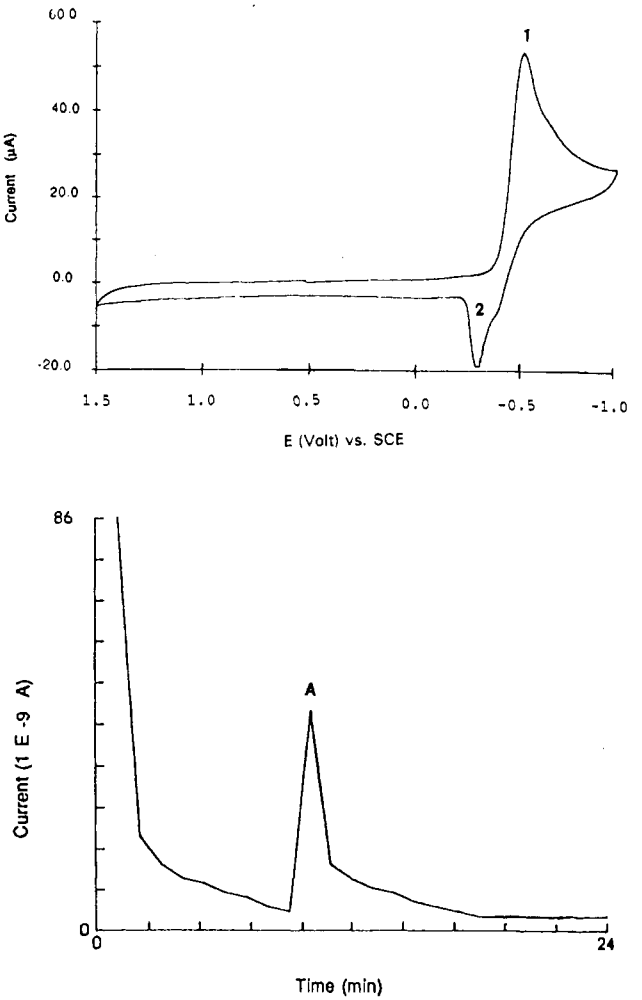

Figure 3. Cyclic voltammogram of 0.0030 M $SnCl_2 \cdot 2H_2O$ in 0.6 M $NaClO_4$, acidified to pH = 2.0 at a scan rate of 100 mV/s: (a, top) potential range of +1.5 to −1.0 V; (b, bottom) bulk electrolysis of a 0.58 M $NaClO_4$ aqueous solution, pH = 2.0. A 1.0-mL aliquot of 0.0042 M $SnCl_2 \cdot 2H_2O$ was injected at point A, demonstrating that observation of a current for the oxidation of stannous chloride is possible.

$Sn(ECD)_2$, based on the synthetic data under conditions of relatively high pH. Formation of $Sn(ECD)Cl_2$ is also possible and the synthesis and crystal structure of this complex has been previously described.[5] The coordination geometry of the tin atom in $Sn(ECD)Cl_2$ is a six-coordinate distorted octahedral which is typical of tin(IV) species.[27] The coordination site consists of the N_2S_2 unit of ECD^{2-} and the two chlorides. Similar to the results obtained for the stannous complex $Sn(CEE)_2$, the coordinated nitrogens of ECD^{2-} are not deprotonated.

The reaction of tin(IV) with HCEE was also monitored by spectrophotometric titrations and the results are similar to the H_2ECD data at low pH. The formation of more than one species is indicated by significant curvature in the plot of absorbance at λ = 245 nm vs the ratio of tin to ligand. Similar experiments were not performed at higher pH values for tin(IV) with HCEE.

Electrochemistry of $SnCl_2 \cdot 2H_2O$. Reduction. The reduction of SnX_2 has been extensively investigated via polarography,[6,30] and the two-electron reduction of Sn^{II} to Sn(Hg) has been established in a variety of supporting electrolytes and is given in eq 1, where X is an anionic ligand or counterion.

$$Sn(X)_2 + 2e^- \rightleftharpoons Sn(Hg) + 2X^- \quad (1)$$

Figure 3 is a representative cyclic voltammogram of $SnCl_2 \cdot 2H_2O$ at a platinum electrode which demonstrates the presence of a reduction wave (wave 1, Figure 3a) and a small oxidation

(27) Donaldson, J. D.; Grimes, S. M. In *Chemistry of Tin*; Harrison, P. G., Ed.; Chapman and Hall, Inc.: New York, 1989; pp 121, 136.
(28) Wells, A. F. *Structural Inorg. Chemistry*, 5th ed.; Clarendon Press: Oxford, England, 1985; p 1183.
(29) (a) Bates, P. A.; Hursthouse, M. B.; Davies, A. G.; Slater, S. D. *J. Organomet. Chem.* **1989**, *363*, 45–60. (b) Betterman, G.; Arduengo, A. J. *J. Am. Chem. Soc.* **1988**, *110*, 877–879. (c) Engelhardt, L. M.; Jolly, B. S.; Lappert, M. F.; Raston, C. L.; White, A. H. *J. Chem. Soc., Chem. Commun.* **1988**, 336–338. (d) Donaldson, J. D.; Grimes, S. M.; Calogero, S.; Russo, U.; Valle, G.; Smith, P. *J. Inorg. Chim. Acta* **1984**, *84*, 173–177. (e) Harrison, P. G.; Haylett, B. J.; King, T. J. *Inorg. Chim. Acta* **1983**, *75*, 259–264. (f) Archer, S. J.; Koch, K. R.; Schmidt, S. *Inorg. Chim. Acta* **1987**, *126*, 209. (g) Olmstead, M. M.; Power, P. P. *Inorg. Chem.* **1984**, *23*, 413.
(30) Avaca, L. A.; Gonzalez, E. R.; Stradiotto, N. R. *J. Electroanal. Chem. Interfacial Electrochem.* **1981**, *130*, 255.

wave (wave 2, Figure 3a). E_{pc} for wave 1 is −0.53 V vs SCE at 100 mV/s and $E_p - E_{p/2}$ is 90 mV. The reduction of the proton is at −0.47 ± 0.04 V under these conditions, but the current for this process is not significant compared to the current observed for the reduction of the stannous species. The smaller than expected current found for the reduction of the proton has been shown to be due to the presence of tin ions.[12] Either tin(II) or tin(IV) ions dramatically inhibit the reduction of proton on a platinum electrode, presumably due to the presence of a tin surface film.[12]

The value of $E_p - E_{p/2}$ of 90 mV is significantly larger than the approximate 30 or 60 mV expected for a simple two- or one-electron process, respectively.[15] The larger value of $E_p - E_{p/2}$ is not due to internal resistance, since a value of 71 mV is found for the $[Fe(CN)_6]^{3-/4-}$ standard. Wave 1 shifts to negative potentials with increasing scan rate and is diffusion controlled, evidenced by a constant value of $i_p/v^{1/2}$. Rotating disk voltammetry gives a total of two electrons for wave 1 by comparison with a ferricyanide standard, after correction for the presence of the proton, assuming similar values for the diffusion coefficients of ferricyanide and tin(II) chloride. No significant change in the number of electrons was found upon changing the rotation rate from 300 to 800 rpm. Bulk electrolysis at a potential negative of wave 1 results in 2.25 ± 0.5 electrons transferred, and after electrolysis formation of Sn metal is observed on the platinum-grid working electrode.

These observations are all in general agreement with eq 1, and the electrochemical mechanism is best described as an ECE(C) process. This is evident from the negative shift of wave 1 combined with the large value of $E_p - E_{p/2}$ in the cyclic voltammetric experiments, indicating an EC process. The observation of two electrons in the rotating disk and bulk electrolysis experiments further suggest that the mechanism is an ECE process with the possibility of additional coupled chemical reactions. The product of the reduction is ultimately tin metal and chloride ion, as evidenced by formation of tin on the electrode surface during bulk electrolysis experiments.

Waves 1 and 2 are coupled since wave 2 is only present after scanning through wave 1. However, wave 1 and wave 2 are not a reversible process since ΔE_p is 170 mV and the peak current ratio, i_{pc}/i_{pa}, is 3.0. Wave 2 is not diffusion controlled, suggesting a surface-localized species. E_{pa} for wave 2 is −0.36 V vs SCE and is independent of scan rate, and the value of $E_p - E_{p/2}$ is 38 mV. Only waves 1 and 2 are observed in multiple-scan experiments which imply that $SnCl_2$ is regenerated by scanning through wave 2. On the basis of this data, wave 2 is assigned to the reoxidation of Sn metal with the ultimate formation of $SnCl_2$. This was confirmed by voltammetric analysis of authentic samples of tin metal.

Oxidation of $SnCl_2 \cdot 2H_2O$. Although Sn(II) solutions are known to readily oxidize upon exposure to air, no oxidation wave is observed for *any* scanning voltammetric method under our general conditions (0.005 M HCl, 0.4 M $NaClO_4$). The failure to observe an oxidation process under these conditions is due to the adsorption of tin(II) chloride on the platinum surface which inhibits a proposed inner-sphere oxidation mechanism for the tin species in solution.[13] The adsorption of $SnCl_2$ on the electrode can be inhibited, and for example, at high chloride conditions (0.005 M HCl, 6.0 M NaCl) we find an oxidation wave for tin(II) to tin(IV) by cyclic voltammetry at E_{pa} = 0.44 V vs SCE at a scan rate of 100 mV/s. This is in general agreement with data reported for the oxidation of Sn(II) to Sn(IV) with other specific interacting supporting electrolytes and/or solution conditions.[6,7,9,13,31] However, the conditions that allow voltammetric measurements of the oxidation of $SnCl_2$ interfere with the coordination reactions that are the focus of the present study.

It is possible to observe a current for the oxidation of tin(II) to tin(IV) under our general conditions, if the time scale of the experiment is slowed down and the background current is compensated. This is shown in Figure 3b, which is the result of a bulk electrolysis experiment at 0.90 V vs SCE in which tin(II) chloride is injected to the solution at point A. The injection is well past the time required for the current to reach baseline levels and a strong current response is observed. A similar injection of a blank solution results in no significant increase in the current. Current is observed under these conditions since the applied potential is now greater than the oxidation potential of $SnCl_2$, and hence, the kinetics for the oxidation process are increased.[13] In principle, one could obtain a value of $E_{1/2}$ from such an experiment by progressively increasing the potential set to the working electrode, injecting a constant amount of tin(II), and plotting the resulting current vs applied potential. However, similar information can also be obtained from a double-step chronocoulometric experiment.

Figure 4a illustrates a double-step chronocoulometric experiment. A potential that is less than the potential required for a given electron transfer ($E^{\circ\prime}$) is set as the initial potential, E_i. A final potential, E_f, greater than the potential for electron transfer and a pulse width, T, are also set. The experiment begins by starting at E_i and stepping to E_f while the current response for time T is monitored. The potential is then stepped back to E_i, and the current response is again monitored for time T. This current is integrated and can be graphed as Q vs T, as shown in Figure 4a. In the case of an oxidation process where there is no rereduction wave, the current measured from E_i to E_f (step 1) contains both faradaic and background current while the current measured from E_f to E_i (step 2) has no faradaic component and consequently gives a measure of the background current. Therefore, compensation for the background current in step 1 can be achieved by subtracting the current of step 2 from the current of step 1. The result is predominantly the current due to the faradaic process of interest.

We have found that by keeping E_i constant and changing E_f to increasingly more positive or negative potentials, the potential for electron transfer can be deduced for processes that do not have a "reversible" electron-transfer process. This is achieved by plotting $Q_1 - Q_2$ (ΔQ) vs E_f. The result is a plot that resembles a polarogram, and thus the potential of electron transfer, E_{cm}, can be determined in a manner similar to $E_{1/2}$, where E_{cm} represents the potential extracted from the chronocoulometry method.

This method was tested with the standard $[Fe(CN)_6]^{3-/4-}$ and hydroquinone/quinone couples. The electron-transfer properties for each of these species are well established and are available in most electrochemical texts.[15] The results for $[Fe(CN)_6]^{3-/4-}$ are a straight-line plot of ΔQ vs E_f (slope of zero) since it is a reversible couple, and hence ΔQ is near 0, independent of E_f. The results for the hydroquinone/quinone standard show the applicability of this technique to "irreversible processes" (i.e. $i_{pa} \neq i_{pc}$), as demonstrated in Figure 4b,c. Figure 4b shows a representative cyclic voltammogram of the oxidation of hydroquinone in aqueous $NaClO_4$ solution, pH near 5. Under our conditions, the value of E_{pa} is 0.61 V vs SCE at 100 mV/s. The results of the chronocoulometric method are shown in Figure 4c. From the plot of ΔQ vs E_f a value of E_{cm} of 0.62 V vs SCE is obtained.

Figure 4d is a representative plot of ΔQ vs E_f for $Sn^{II}Cl_2 \cdot 2H_2O$ in $NaClO_4/H_2O$, acidified to pH 2.0. The value of E_{cm} for the oxidation is determined to be 0.06 V ± 0.04 vs SCE. Thin-layer bulk electrolysis (TLBE) methods were used to support the chronocoulometric results by performing electrolysis at different potentials and comparing the amount of current passed as a function of potential. The TLBE data confirmed the current increase in the same potential range. The value of E_{cm}, however, is significantly less positive than the E_{pa} of 0.44 V measured by cyclic voltammetry under the conditions of 6 M NaCl.

Ligand Addition to $SnCl_2 \cdot 2H_2O$. The ligand addition reactions of $SnCl_2 \cdot 2H_2O$ with both H_2ECD and HCEE to form Sn(ECD) and $Sn(CEE)_2$, respectively, were examined by both the chronocoulometric experiments to determine the effect of ligation on the oxidation potential and by titration experiments monitored by cathodic scans in the cyclic voltammograms (wave 1) to examine the coordination reactions. Cyclic voltammograms and the chronocoulometric experiment were performed on both H_2ECD

(31) DeSesa, M. A.; Hume, D. N.; Glamm, A. C.; DeFord, D. D. *Anal. Chem.* **1953**, *25*, 983.

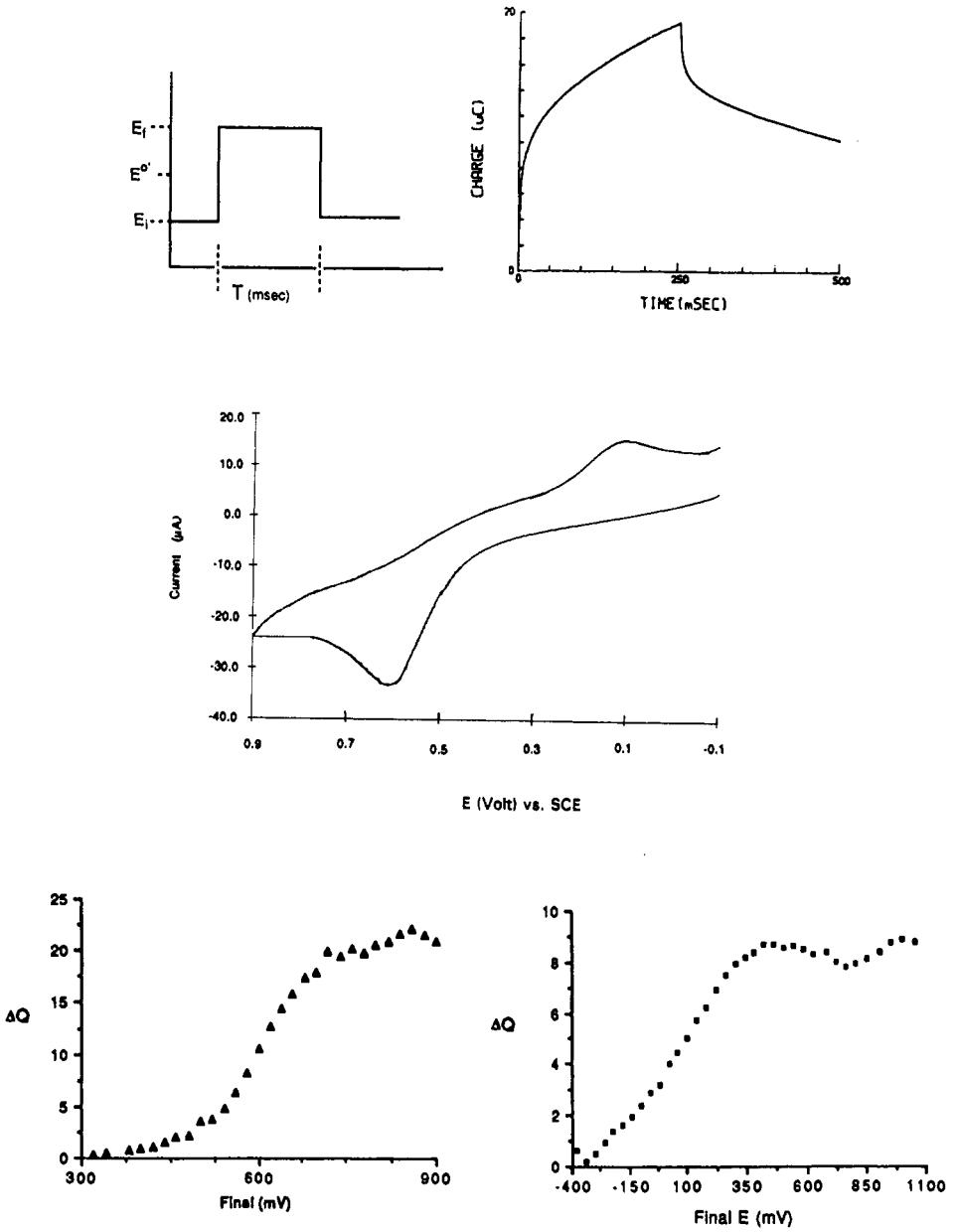

Figure 4. (a, Top) step function of a double-step chronocoulometry experiment and corresponding response. The solution used for the experiment was 0.0044 M $Sn^{II}Cl_2 \cdot 2H_2O$ in 0.4 M $NaClO_4$, acidified to pH = 2.0. (b, Middle) cyclic voltammogram of 0.0093 M hydroquinone in 0.7 M $NaClO_4$ at a scan rate of 100 mV/s. (c, Bottom left) plot of ΔQ (μC) vs E_f (mV) of 0.0093 M hydroquinone in 0.7 M $NaClO_4$, E_i = 0.30 V. (d, Bottom right) plot of ΔQ (μC) vs E_f (mV) of 0.0049 M $Sn^{II}Cl_2 \cdot 2H_2O$ in 0.4 M $NaClO_4$, pH = 2.0. E_i = −0.35 V.

and HCEE in the absence of tin as a blank. In all cases, no waves of any significance were observed for these ligands.

The effect of formation of Sn(ECD) and $Sn(CEE)_2$ was determined by the chronocoulometry method and plots of ΔQ vs E_f demonstrate a value of E_{cm} of 0.15 ± 0.06 and 0.43 ± 0.06 V vs SCE for Sn(ECD) and $Sn(CEE)_2$, respectively. Hence, formation of Sn(ECD) causes only a slight positive change in the oxidation potential while formation of $Sn(CEE)_2$ causes a relatively large positive shift in oxidation potential.

The addition of a ligand to a metal complex can be investigated by monitoring the shift in the peak potential for electron transfer to/from the metal species as the concentration of complexing ligand is increased. This has been used to examine ligand addition reactions of several metal compounds,[23,32] especially metalloporphyrins.[33-35] The cyclic voltammetric response for our system indicates that upon formation of the complex, wave 1 shifts to positive potentials while the potential for wave 2 does not significantly change. Observation of wave 2 means that tin metal is also formed upon reduction of either Sn(ECD) or $Sn(CEE)_2$. Hence the general electron-transfer reaction for both complexes can be described as either an ECE or an EEC process.

Titration experiments with tin(II) chloride were performed in which the shift in wave 1 was monitored upon the addition of either H_2ECD or HCEE. The data for addition of H_2ECD yields a slope of −35 mV/log [L] (correlation coefficient of 0.91), while titration with HCEE gives a slope of −50 mV/log [L] (correlation coefficient of 0.85). Given that n is 2, these data suggest one H_2ECD and two HCEE ligands are added in the complexation reaction. This is in general agreement with the results of the spectrophotometric and synthetic studies. The scatter in the plots is due to several experimental difficulties, the most significant of which is performing a titration experiment with relatively low concentra-

(32) Boyd, D. C.; Rodman, G. S.; Mann, K. R. *J. Am. Chem. Soc.* **1986**, *108*, 1779.
(33) Kadish, K. M. *Prog. Inorg. Chem.* **1986**, *34*, 435.
(34) Cornillon, J.-L.; Anderson, J. E.; Kadish, K. M. *Inorg. Chem.* **1986**, *25*, 2611.
(35) Kadish, K. M.; Bottomley, L. A.; Cheng, J. S. *J. Am. Chem. Soc.* **1978**, *100*, 2732.

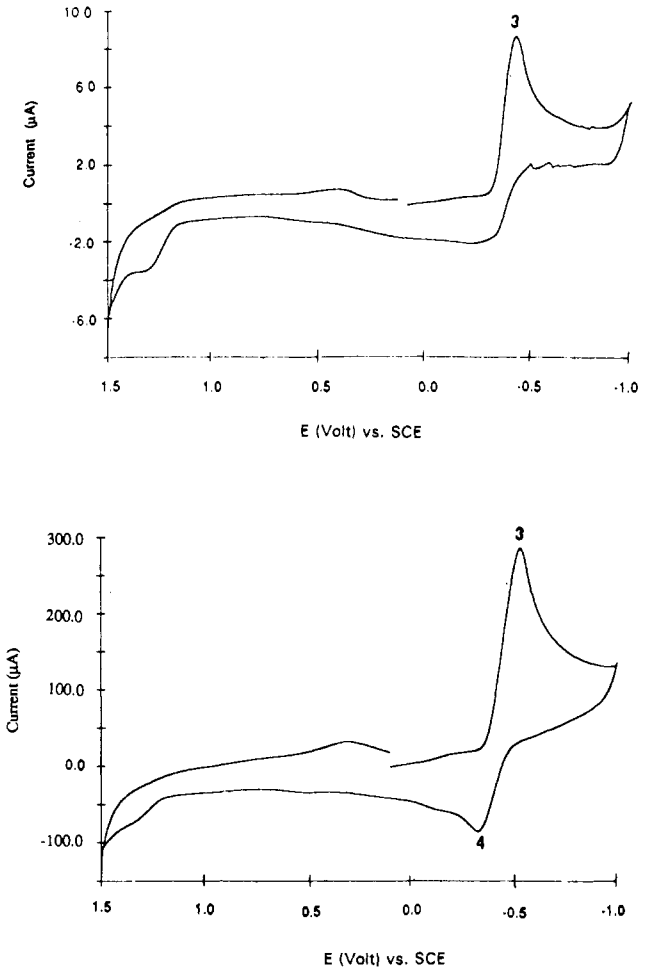

Figure 5. (a, Top) cyclic voltammogram of 0.0028 M $SnCl_4 \cdot 5H_2O$ in 0.4 M $NaClO_4$ acidified to pH = 2.0, at a scan rate of 100 mV/s and a range of +1500 to -1000 mV. (b, Bottom) cyclic voltammogram of 0.0028 M $Sn^{IV}Cl_4 \cdot 5H_2O$ in 0.4 M $NaClO_4$ acidified to pH = 2.0, at a scan rate of 1000 mV/s and a range of +1500 to -1000 mV.

tions of air-sensitive species. Upon addition of L there is also a systematic change in the electrochemical characteristics of wave 1 such as an increase in i_p and a decrease in $E_p - E_{p/2}$. For example, when the molar ratio of H_2ECD to tin is 2 to 1, the value of $E_p - E_{p/2}$ for wave 1 is approximately 40 mV compared to the value of 90 mV in the absence of added ligand. Similar results are found when the added ligand is HCEE. The change in $E_p - E_{p/2}$ could be due to several factors such as a change from the ECE mechanism for the reduction of $SnCl_2$ to an EEC mechanism for reduction of the complex. Other possibilities are that the change in $E_p - E_{p/2}$ is due to the shift in $E°$ upon formation of the complex or that the chemical reaction coupled to the electron transfer in the ECE step is faster for the complex than for tin chloride.

Electrochemistry of $SnCl_4 \cdot 5H_2O$. Electrochemical investigations of $SnCl_4 \cdot 5H_2O$ with aqueous solutions are discussed in the literature.[6,9] Two polarographic waves are observed for the reduction of $SnCl_4 \cdot 5H_2O$ and have been assigned to the sequential formation of Sn(II) and tin metal at chloride concentrations of 0.5 M and greater.[6] The first wave is irreversible and is proposed to consist of a rate-determining step involving the formation of a tin(III) species.[6,9] Under conditions of relatively low chloride ion concentrations, one wave is observed for the reduction of tin(IV) to tin metal.

A cyclic voltammogram of $SnCl_4 \cdot 5H_2O$ is shown in Figure 5a. A diffusion-controlled reduction wave (wave 3, Figure 5a) at an E_{pc} of -0.44 V vs SCE at 100 mV/s is found with no coupled return wave and a value for $E_p - E_{p/2}$ of 60 mV. Again the reduction of the proton is inhibited,[12] and the current due to this process is much less than that found for the reduction of tin(IV). The value of E_p for the reduction of $SnCl_4$ is 0.09 V less negative than that for $SnCl_2$. This suggests an easier reduction of the tin(IV) species, which is fully consistent with the higher oxidation state of the metal ion.

The value of E_{pc} for wave 3 shifts to more negative potentials with increasing scan rate. The voltammetric response is scan rate dependent, as shown in Figure 5b, which is the response obtained at 1000 mV/s. In this case there is a small return wave (wave 4, Figure 5b) after scanning through the reduction, suggesting the presence of a short-lived intermediate. Bulk electrolysis at a potential negative of wave 3 results in four electrons transferred per tin species after correction for the presence of the proton. However, there is no indication of formation of tin on the electrode in the bulk electrolysis experiments either visually or by electrochemical methods.

The electrochemical data indicate that the reduction of $SnCl_4 \cdot 5H_2O$ in aqueous solution is a four-electron process with coupled chemical reactions. Peak analysis of the cyclic voltammetric data suggests a one-electron reduction as the rate-limiting step, but the value of $E_p - E_{p/2}$ could also be a deceptive coincidence. A one-electron step would be in agreement with the mechanisms in the literature, suggesting formation of a tin(III) species.

Ligand Addition to $SnCl_4 \cdot 5H_2O$. The ligand addition reactions of H_2ECD and HCEE to $SnCl_4 \cdot 5H_2O$ were also investigated. The peak potential shifts in a negative direction with an increasing concentration of H_2ECD or HCEE, opposite to what is observed upon addition of these ligands to $SnCl_2 \cdot 2H_2O$. The corresponding plot of peak potential as a function of the log of the ligand concentration gives a straight line with a slope of 82 and 31 mV/log [L] for H_2ECD and HCEE, respectively.[36] Analysis of these data is not possible since more than one tin(IV) complex is known to form upon addition of L based on the photometric studies and since the electron-transfer mechanism is complicated. However, the data do show that there is a significant change in the reductive properties of tin(IV) upon reaction with L.

Nonaqueous Electrochemistry of $Sn(ECD)Cl_2$. The complex $Sn(ECD)Cl_2$ is not sufficiently soluble in water to perform electroanalysis. However, in both acetonitrile and methylene chloride electrochemical results could be obtained and these results are reported below. The analysis of $SnCl_2 \cdot 2H_2O$ and $SnCl_4 \cdot 5H_2O$ was also performed in acetonitrile to permit identification of reduction product of $Sn(ECD)Cl_2$ as tin metal.

Figure 6a is a typical cyclic voltammogram of $Sn(ECD)Cl_2$ in acetonitrile with TBAP as the supporting electrolyte. As shown, there is a reduction process, wave 5, with a value of E_{pc} of -1.72 V vs SCE at 100 mV/s. The value of $E_p - E_{p/2}$ is 100 mV and the process is diffusion controlled. Wave 5 shifts negative with increasing scan rate, which, in combination with the value of $E_p - E_{p/2}$, suggests a multiple-electron-transfer process with coupled chemical reactions. A small return wave (wave 6) at E_{pa} of -0.65 V at 100 mV/s is indicated after scanning negative of wave 5, as shown in Figure 6a. However, the predominant process after scanning negative of wave 5 is a strong oxidation peak at 0.05 V vs SCE (wave 7, Figure 6a). Wave 7 is not a diffusion-controlled process and combined with wave analysis is assigned to a surface-localized species.

Figure 6b shows the electrochemical response obtained for the reduction of solutions of $SnCl_4 \cdot 5H_2O$ in acetonitrile. There are four reduction processs (waves 8-11, Figure 6b) under these conditions. Individual analysis of these waves would be difficult, considering that $SnCl_4 \cdot 5H_2O$ is known to undergo substitution by acetonitrile.[37-39] However, of note is that wave 7 is found on the return scans in the cyclic voltammogram. Wave 7 is also found in the cyclic voltammograms of stannous chloride in acetonitrile.

(36) Correlation coefficients for L = H_2ECD and HCEE were 0.96 and 0.84, respectively.
(37) Thomas, F. G.; Kolthoff, I. M. *J. Electroanal. Chem. Interfacial Electrochem.* **1971**, *31*, 423.
(38) Avaca, L. A.; Gonzalez, E. R.; Stradiotto, N. R. *J. Electroanal. Chem. Interfacial Electrochem.* **1981**, *130*, 255.
(39) Webster, M.; Blayden, H. E. *J. Chem. Soc. A* **1969**, 2443.

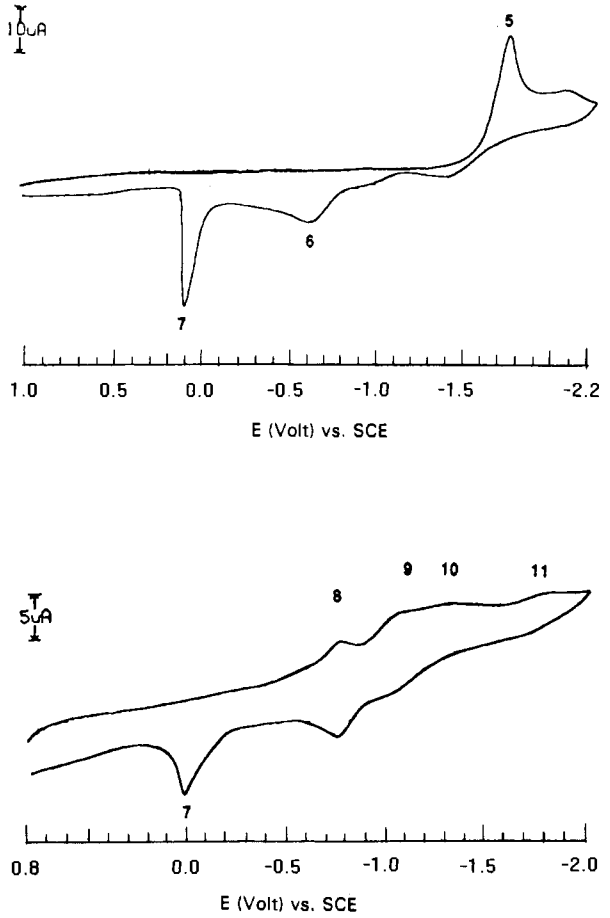

Figure 6. (a, Top) cyclic voltammogram of 0.0050 M $Sn(ECD)Cl_2$ in 0.00 M TBAP, acetonitrile solution at a scan rate of 100 mV/s. (b, Bottom) cyclic voltammogram of 0.0078 M $SnCl_4 \cdot 5H_2O$ in 0.11 M TBAP, acetonitrile solution at a scan rate of 100 mV/s.

This implies that a common species is formed in the reduction of solutions of $Sn(ECD)Cl_2$ and $SnCl_4$ and $SnCl_2$, and on the basis of coulometric data for $SnCl_4 \cdot 5H_2O$ and $SnCl_2 \cdot 2H_2O$, this wave is assigned to be due to the oxidation of tin metal.

Similar results are found for the reduction of $Sn(ECD)Cl_2$ when methylene chloride is the solvent. In this case, wave 5 has an E_{pc} of −1.63 V vs SCE at 100 mV/s. Wave 5 is again a diffusion-controlled process with a value of $E_{pc} - E_{pc/2}$ of 214 mV. A negative shift in the value of E_{pc} is found upon increasing the scan rate, and multiple scans suggest passivation of the electrode surface occurs during the reduction process. In agreement with passivation of the electrode surface upon reduction of $Sn(ECD)Cl_2$, no oxidation waves are found in return scans of the cyclic voltammetric experiment after scanning negative of wave 5 in methylene chloride.

Conclusions. The Sn(II) and Sn(IV) compounds prepared in this study and elsewhere[5] yield complexes characteristic of each of the two oxidation states. The Sn(II) complexes with H_2ECD and HCEE are Sn(ECD) and $Sn(CEE)_2$ in both solution and the solid state, whereas a variety of complexes are formed with Sn(IV) ions. With both ligands, a Sn(II) complex is formed with a N_2S_2 inner coordination sphere, as demonstrated by the crystal structure determination of $Sn(CEE)_2$. An important difference between the two ligands, however, is the connectivity of the ligating group. The structure of $Sn(CEE)_2$ shows a trans orientation of the nitrogen and sulfur atoms; the ECD ligand cannot coordinate in this fashion. In addition, the ECD ligand is tetradentate and will therefore restrict the binding of the N_2S_2 groups to the metal ion; the CEE ligands will not be under the same restrictions.

As determined by the chronocoulometric experiment, there was a difference of 280 mV between the oxidation potential for $Sn(CEE)_2$ and Sn(ECD) and a difference of 370 mV between the oxidation of $Sn(CEE)_2$ and $SnCl_2 \cdot 2H_2O$. The difference between $Sn(CEE)_2$ and Sn(ECD) is large, given the close nature of the two different ligands, and demonstrates that the speciation of tin(II) can have a significant effect on the reducing ability of the stannous species. Although this effect is not surprising, it is the first time that the magnitude of the shift in oxidation potential upon ligation of tin(II) has been measured with ligands relevant to radiopharmaceuticals. Depending upon the reduction potential of the target species, such as TcO_4^- for radiopharmaceuticals, such a shift could have a significant effect.

Acknowledgment. The preparation of $Sn(ECD)_2$ was developed by L. Maheu and R. Jones, E. I. du Pont de Nemours and Co., Inc., Wilmington, DE, and S. Cyr, Du Pont Merck Pharmaceutical Co., assisted with the tin(II) and tin(IV) spectrophotometric titration studies. J.E.A. acknowledges E. I. du Pont de Nemours for support of this research.

Supplementary Material Available: Listings of crystallographic data (Table S1), thermal parameters (Table S2), hydrogen atom positions (Table S3), and all bond distances and angles (Table S4) (5 pages); a listing of observed and calculated structure factors (Table S5) (6 pages). Ordering information is given on any current masthead page.